

See discussions, stats, and author profiles for this publication at: <https://www.researchgate.net/publication/253885596>

Vibrational Dependence of Excited State Intramolecular Proton Transfer in 2-(2'-PYRIDYL)PYRROLE in the Gas Phase via High Resolution Electronic Spectroscopy

ARTICLE · JUNE 2010

READS

20

5 AUTHORS, INCLUDING:



Adam J Fleisher

National Institute of Standards and Technol...

42 PUBLICATIONS 132 CITATIONS

SEE PROFILE



David W. Pratt

University of Vermont

231 PUBLICATIONS 4,317 CITATIONS

SEE PROFILE



Michał Kijak

Instytut Chemii Fizycznej PAN

25 PUBLICATIONS 198 CITATIONS

SEE PROFILE



J. Waluk

Polish Academy of Sciences

258 PUBLICATIONS 3,720 CITATIONS

SEE PROFILE

Excited-State Proton Transfer in *syn*-2-(2'-Pyridyl)pyrrole Occurs on the Nanosecond Time Scale in the Gas Phase

Philip J. Morgan, Adam J. Fleisher, Vanesa Vaquero-Vara, and David W. Pratt*


Department of Chemistry, University of Pittsburgh, Pittsburgh, Pennsylvania 15260, United States

Randolph P. Thummel

Department of Chemistry, University of Houston, Houston, Texas 77204, United States

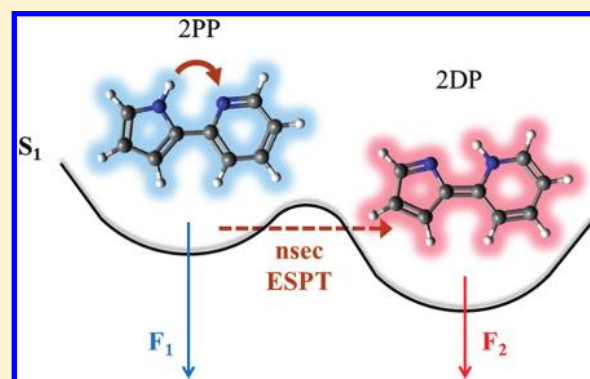
Michał Kijak and Jacek Waluk

Institute of Physical Chemistry, Polish Academy of Sciences, Kasprzaka 44/52 01-224 Warsaw, Poland

 Supporting Information

ABSTRACT: Microwave and UV excitation spectra of 2-(2'-pyridyl)pyrrole (2PP) have been recorded at high resolution in the gas phase. Analyses of these data show that the *syn* conformer of 2PP is a planar molecule in both the ground (S_0) and first excited (S_1) electronic states, and that the S_1 state undergoes a relatively slow excited-state proton transfer (ESPT) reaction when excited by light, as measured by the homogeneous line broadening that is observed in its UV spectrum. Apparently, excitation of the S_1 state moves electronic charge from the pyrrole ring to the pyridine ring, but the simultaneous transfer of the proton is inhibited by an unfavorably oriented dipole under solvent-free conditions. The rate of the ESPT reaction is enhanced by more than an order of magnitude with simultaneous excitation of a 144 cm^{-1} in-plane vibrational mode.

SECTION: Dynamics, Clusters, Excited States



We wish to report the observation of homogeneous line broadening in the high-resolution fluorescence excitation spectrum of *syn*-2-(2'-pyridyl)pyrrole (2PP) in the gas phase, which makes possible the measurement of the rate of an excited-state hydrogen atom transfer reaction in the isolated molecule, free of the perturbations of external solvent molecules.

Interest remains high in reactions of this type, loosely referred to as excited-state proton transfer (ESPT) reactions,¹ since the pioneering study of Herek, et al.² on methyl salicylate (MS). Relevant recent experiments include studies of 2-(2'-hydroxyphenyl)-5-phenyloxazole (HPPO),³ the 7-azaindole (7AI) dimer,⁴ methanol complexes of 7-hydroxyquinoline (HYQ),⁵ and water complexes of 7AI.⁶ However, in all of these cases except the first, the course of the ESPT reaction was monitored by the appearance of a red-shifted emission of the product on short time scales, following picosecond (or less) pulsed excitation of the reactant, leading to ambiguities concerning the nature of the prepared state. Only in HPPO was homogeneous line broadening observed, from which an ESPT rate was determined, but even in this case excitation was provided by a nanosecond pulsed Nd:YAG pumped dye laser having a large bandwidth.³ Thus, as will become apparent, all of

the cited experiments utilized excitation sources whose frequency and/or coherence widths are much larger than the homogeneous widths of individual rovibronic transitions in the $S_1 \leftarrow S_0$ electronic spectrum of 2PP.

Our experiments were performed in the collision-free environments of a supersonic jet for the microwave experiments (using a chirped-pulse Fourier transform microwave (CP-FTMW) spectrometer)⁷ and a molecular beam for the UV experiments using a $\sim 1\text{ MHz}$ (0.00003 cm^{-1}) wide laser.⁸ Previous studies of 2PP⁹ have shown that the isolated molecule exhibits dual fluorescence, a strong "normal" fluorescence (F_1) that is attributed to 2PP (see structure I), and a much weaker red-shifted emission (F_2) that is attributed to the tautomer of 2PP, 1,2-dihydro-2-(2H-pyrrol-2-ylidene)-pyridine (2DP, structure II). The maximum of F_1 in the jet is blue-shifted with respect to the solution value, but the maximum of F_2 appears at the same wavelength in both the gas phase and in solution.

Received: June 29, 2011

Accepted: August 2, 2011

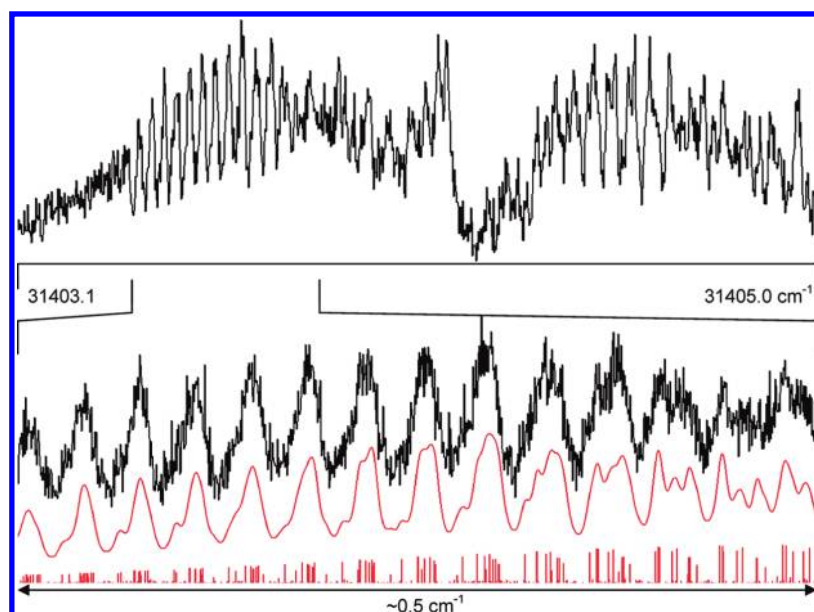


Figure 1. Rotationally resolved fluorescence excitation spectrum of the origin band in the S_1-S_0 electronic transition of 2PP in the gas phase, at ~ 318 nm. The lower part of the figure shows an expanded scale view of a portion of the P-branch region. The black trace is the experimental spectrum, and the red trace is the simulated spectrum, with and without a convoluted line shape function; the vertical lines represent the individual rovibronic transitions responsible for the spectrum.

Scheme 1. Structures of 2PP(I) and 2DP(II)

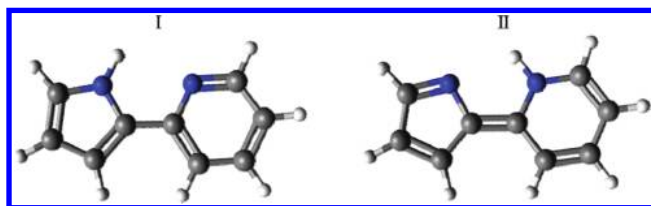


Figure 1 shows the high-resolution S_1-S_0 fluorescence excitation spectrum of the origin band of 2PP, recorded in a molecular beam by monitoring the total emission following excitation at ~ 318 nm with the narrow-band laser. Immediately apparent is the partially resolved rotational structure in the spectrum. This was analyzed using the following procedure. First, ground-state rotational constants of 2PP were determined from a fit to Watson's A-reduced Hamiltonian¹⁰ of nine measured μ_a -type transitions in an independently measured microwave spectrum. (No μ_b - or μ_c -type transitions were observed in this spectrum.) Next, excited-state rotational constants of 2PP were determined from a fit to rigid-rotor Hamiltonians of the observed rotational structure in the UV spectrum in Figure 1 using the program jB95.¹¹ In this fit, ground-state constants were kept fixed to their microwave values, and excited-state constants were varied in a least-squares fashion to minimize differences between observed and calculated frequencies. Ultimately, 70 individual rovibronic transitions were fit, with a standard deviation of 4.9 MHz at a rotational temperature of ~ 5 K. Finally, each of the individual features in the spectrum was fit using a Voigt line shape profile, resulting in a Gaussian width of 18–20 MHz, a Lorentzian width of 210 ± 20 MHz, and an overall band character that is 90% a -type and 10% b -type, giving an electronic transition moment that makes an angle of $\theta = \pm 18 \pm 5^\circ$ with respect to the a inertial axis of the 2PP frame.

Tables 1 and 2 list the rotational constants that were derived from this analysis and compares them with selected theoretical values.¹² First, we note the excellent agreement between experiment and theory for the ground electronic state of 2PP (Table 1); the calculated values of A , B , and C are nearly identical to the measured ones, especially when zero-point vibrational motions are taken into account. 2PP is a planar molecule in its ground electronic state. The calculated permanent electric dipole moment (EDM) of 2PP also accords with experiment; μ makes its largest projection on the a -inertial axis ($\mu_a = -1.38$ D), thereby explaining the absence of strong μ_b - and μ_c -type transitions in the microwave spectrum, and (according to theory) points toward the pyrrole ring. The predicted values of the rotational constants

Table 1. Inertial Parameters of 2PP in Its Ground Electronic State^a

parameter	2PP microwave	2PP theoretical ^b	2DP theoretical ^b
A (MHz)	3561.72(22)	3575.6	3513.2
B (MHz)	710.4228(14)	711.8	724.2
C (MHz)	592.5936(14)	593.9	600.6
ΔI ($\text{u}\text{\AA}^2$)	$-0.444(12)$	-0.41	-0.28
μ_a (D)		-1.38	-5.37
μ_b (D)		0.11	0.37
$ \mu $ (D)		1.38	5.38
OMC (kHz)	14		
assigned lines	9		

^a Standard deviations in the final digits are shown in parentheses.

^b Geometry optimization calculations, which include zero-point vibrational level contributions in S_0 , were done at the M05-2X/6-31+G* level of theory using anharmonic frequency corrections. Permanent electric dipoles were calculated using an MP2/aug-cc-pVDZ point calculation on the previously optimized vibrationally averaged geometry.

Table 2. Inertial Parameters of 2PP in Its Excited Electronic State^a

parameter	2PP origin band	2PP theoretical ^b	2DP theoretical ^b
A (MHz)	3427.5(1.0)	3481.1	3495.6
B (MHz)	725.72(10)	724.9	726.7
C (MHz)	599.22(10)	600.3	602.1
ΔI (uÅ ²)	−0.43(28)	−0.42	−0.61
μ_a (D)		1.20	−0.94
μ_b (D)		−0.06	0.22
$ \mu $ (D)		1.21	0.97
origin (cm ^{−1})	31404.1		
a/b/c type	90/10/0	99/1/0	86/14/0
OMC (MHz)	4.9		
assigned lines	70		

^a Standard deviations in the final digits are shown in parentheses.

^b Geometry optimization calculations, which include zero-point vibrational level contributions in S_1 , were done at the CIS/6-31+G* level of theory using anharmonic frequency corrections. Permanent electric dipoles were calculated using a CIS/aug-cc-pVDZ point calculation on the previously optimized vibrationally averaged geometry.

and EDM of the proton transferred structure, 2DP, in its ground electronic state are significantly different from those of 2PP.

Next, we consider the properties of the excited electronic state (Table 2). Here, the agreement between the experimental and calculated rotational constants is less impressive, but it is adequate to conclude that the carrier of the spectrum is the non-proton transferred structure, 2PP, rather than 2DP. This accords with expectations: the F_2 emission makes only a small contribution to the total fluorescence intensity.⁹ 2PP is also a planar molecule in its S_1 state. The large decrease in A (−134 MHz), compared to the ground state, may be attributed to increases in bond lengths perpendicular to a , reflecting expansions of the pyridine and pyrrole rings upon excitation. The small increases in B and C (+15.3 and +6.6 MHz, respectively) indicate that the pyridine and pyrrole rings are moving closer together in the excited state. Theory predicts the C—C bond linking the two rings to have a length of 146 pm in the S_0 state and 139 pm in the S_1 state. The shorter length of this bond in the S_1 state may reveal incipient motion along the ESPT reaction coordinate, as this bond is a double bond in 2DP. Although the F_2 emission is relatively weak, the eigenstates excited in our experiments

may contain small contributions from the proton-transferred structure.

According to theory, the $S_1 \leftarrow S_0$ transition is principally a π, π^* (highest occupied molecular orbital to lowest unoccupied molecular orbital (HOMO—LUMO)) transition that moves electron density from the pyrrole ring to the pyridine ring, strengthening the bond between them. The calculated transition dipole moment (TDM) makes an angle of 5.8° with the a axis, in agreement with experiment. Owing to the motion of charge, theory predicts that direction of the permanent EDM is reversed in the S_1 state of 2PP, but has about the same magnitude; whereas the magnitude of the EDM in the S_1 state of 2DP is greatly reduced, compared to the ground S_0 state, but has the same sign. A similar reversal in sign of the EDM has been observed in the $S_1 \leftarrow S_0$ spectrum of the related molecule, 1-phenylpyrrole (1PhP).¹³

Direct evidence for the ESPT reaction in 2PP is provided by the homogeneous line broadening observed in its high-resolution UV spectrum, 210 MHz, which considerably exceeds the Doppler contribution to the line width of 18–20 MHz. The Lorentzian contribution gives a measured lifetime of 0.80 ± 0.05 ns for the S_1 state. Now, molecules of this type typically exhibit fluorescence lifetimes that are an order of magnitude longer than this. For example, the $S_1 (\pi, \pi^*)$ state of 1PhP has a lifetime of 13 ns.¹³ The calculated oscillator strength of the $S_1 \leftarrow S_0$ transition of 2PP is 0.33,¹⁴ whereas that of 1PhP is substantially less.¹³ Thus, while it is possible that the observed line broadening is caused by an enhanced radiative decay of 2PP, we attribute the increased spectral width of the $S_1 \leftarrow S_0$ origin band of 2PP to an ESPT reaction in the S_1 state.

Proof of this conjecture is provided by the measurement of the high-resolution spectrum of the +144 cm^{−1} vibronic band in the $S_1 \leftarrow S_0$ spectrum of 2PP, shown in Figure 2. This band exhibits significantly broader lines, compared to the origin band in Figure 1. While it proved impossible to assign individual features in the spectrum shown in Figure 2, its overall contour can be simulated with a Lorentzian contribution that is 10 times larger than that of the origin band, giving an S_1 lifetime that is 10 times shorter, 0.08 ns (80 ps). Previous gas phase studies of the low-resolution fluorescence excitation spectrum of 2PP with selective detection of the F_2 emission⁹ revealed a large increase in the relative intensity of this band and other bands built on the 144 cm^{−1} vibration, compared to a spectrum that was detected by monitoring the total emission, suggesting that this vibration is a promoting mode for the ESPT reaction. Thus, the reduced life-

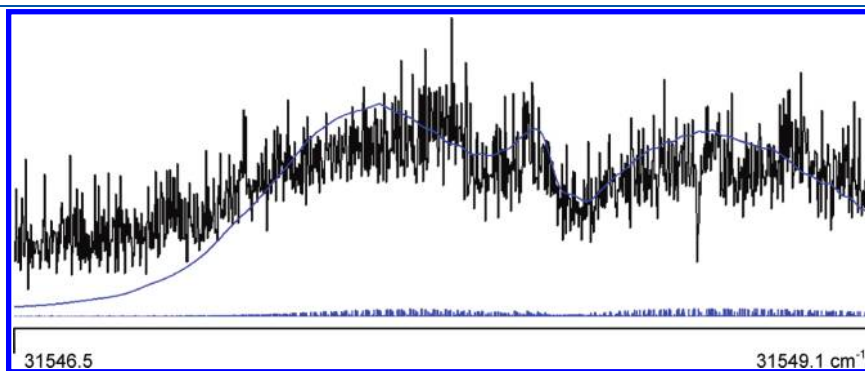


Figure 2. Contour fit of the rotationally resolved fluorescence excitation spectrum of the 0,0 + 144 cm^{−1} vibronic band in the $S_1 \leftarrow S_0$ electronic transition of 2PP. The experimental spectrum is shown in black, and the simulation is shown in blue.

times of both observed vibrational levels in the S_1 state of 2PP may safely be attributed to an ESPT reaction.

Previous studies of 2PP and related molecules in the condensed phase¹⁵ suggest time scales on the order of picoseconds or less for the ESPT reaction. So, it was initially surprising to discover that the reaction rate is considerably slower than this for the isolated molecule in the gas phase. One possible explanation for this result is, of course, that since the previous experiments were performed with picosecond and femtosecond lasers, the molecules were in the statistical limit with respect to the ensuing dynamics. All vibrational modes could be accessed under these conditions, speeding up ESPT. Another possibility is that the process is “solvent-assisted” in the condensed phase. In cyclic water or alcohol complexes of molecules such as 7AI, simulations¹⁶ have shown that very efficient and fast proton-transfer reactions can be expected. However, a recent gas phase study of an isolated 7AI–H₂O complex in the gas phase¹⁷ has revealed that ESPT does not occur within the lifetime of the S_1 state, despite a favorable position of the attached water molecule. In that case, photoexcitation produces “instantaneous” charge transfer, but fast proton transfer does not occur.

Rode and Sobolewski¹⁴ have recently examined the role of electron and proton transfer processes in hydrogen-bonded systems using ab initio methods. In the case of 2PP, they find that the S_1 state of the *syn* conformer shows a small barrier (about 0.2 eV) for transfer of a hydrogen atom to the pyridine ring. A second highly polar charge transfer state of π, π^* character drives the proton transfer, which leads to a conical intersection and ultrafast conversion. However, in the bare molecule, access to this state is blocked by the barrier; the S_1 state of 2DP is a saddle point on the potential energy surface, and is unstable with respect to torsion around the central CC bond. There is no evidence for torsional activity in the low-resolution spectra of 2PP. Instead, we find (as did Kijak, et al.⁹) that an in-plane vibrational mode promotes the process, and that the polarization of the +144 cm⁻¹ band in the S_1 – S_0 spectrum of 2PP is similar to that of the origin band, suggesting that vibronic coupling is not involved. (The important role of vibronic coupling in mediating access to conical intersections has been discussed elsewhere.¹⁸) Thus, from our perspective, the barrier that slows the ESPT process in the isolated molecule is more likely to have its origin in the orientation of its permanent electric dipole.¹⁹ If the dipole moments of the normal and tautomeric forms differ either in their magnitude or in their orientation (or both), a barrier might then exist along the ESPT coordinate in the isolated molecule that cannot be compensated for by solvent reorganization. Our calculations on the present system suggest that the excited-state permanent EDMs of 2PP and 2DP have approximately the same magnitudes but are oriented in opposite directions (see Table 2). The same is true for 7AI–H₂O.¹⁷ Solvent molecules are not required in the salicylic acid/MS systems, since the dipoles of the two connecting states are more nearly aligned, and there is no barrier, even in the isolated molecule.²⁰ Therefore, it is perhaps not surprising that the ESPT reaction of 2PP in the gas phase is significantly slower than the corresponding reaction in solution.

■ ASSOCIATED CONTENT

S Supporting Information. Table S1 lists the observed and calculated frequencies of the pure rotational transitions observed in the microwave experiments. This material is available free of charge via the Internet at <http://pubs.acs.org>.

■ AUTHOR INFORMATION

Corresponding Author

*E-mail: pratt@pitt.edu.

■ ACKNOWLEDGMENT

Some theoretical calculations were performed at the Center for Simulation and Modeling (SAM) at the University of Pittsburgh. This research has been supported by the National Science Foundation (CHE-0714751, RPT, and CHE-0911117, DWP), the Robert E. Welch Foundation (E-621, RPT), and the Andrew Mellon Predoctoral Fellowship Program (AJF). We are grateful for their support.

■ REFERENCES

- (1) *Hydrogen Bonding and Transfer in the Excited State*; Han, K.-L., Zhao, G.-J., Eds.; Wiley-Interscience: New York, 2010.
- (2) Herek, J. L.; Pedersen, S.; Banares, L.; Zewail, A. H. *J. Chem. Phys.* **1992**, *97*, 9046.
- (3) Douhal, A.; Lahmani, F.; Zehnacker-Rentien, A.; Amat-Guerri, F. *J. Phys. Chem.* **1994**, *98*, 12198.
- (4) Folmer, D. E.; Wisniewski, E. S.; Hurley, S. M.; Castleman, A. W., Jr. *Proc. Natl. Acad. Sci. U.S.A.* **1999**, *96*, 12980.
- (5) Matsumoto, Y.; Ebata, T.; Mikami, N. *J. Phys. Chem. A* **2002**, *106*, 5591.
- (6) Pino, G. A.; Alata, I.; Dedonder, C.; Jouvet, C.; Sakota, K.; Sekiya, H. *Phys. Chem. Chem. Phys.* **2011**, *13*, 6325.
- (7) Bird, R. G.; Neill, J. L.; Alstadt, V. J.; Young, J. W.; Pate, B. H.; Pratt, D. W. *J. Phys. Chem. A* **2011**, DOI: 10.1021/jp111075r.
- (8) Majewski, W. A.; Pfanstiel, J. F.; Plusquellic, D. F.; Pratt, D. W. In *Laser Techniques in Chemistry*; Myers, A. B., Rizzo, T. R., Eds.; Techniques of Chemistry Series; John Wiley and Sons: New York, 1995; Vol. XXIII, pp 101–148.
- (9) Kijak, M.; Nosenko, Y.; Singh, A.; Thummel, R. P.; Waluk, J. *J. Am. Chem. Soc.* **2007**, *129*, 2738.
- (10) Watson, J. K. G. In *Vibrational Spectra and Structure*; Durig, J. R., Ed.; Elsevier: Amsterdam, 1977; Vol. 6, pp 1–89.
- (11) Plusquellic, D. F.; Suenram, R. D.; Mate', B.; Jensen, J. O.; Samuels, A. C. *J. Chem. Phys.* **2001**, *115*, 3057.
- (12) Frisch, M. J.; Trucks, G. W.; Schlegel, H. B.; Scuseria, G. E.; Robb, M. A.; Cheeseman, J. R.; Montgomery, J. A., Jr.; Vreven, T.; Burant, J. C.; et al. *Gaussian 03*, revision 6.0; Gaussian, Inc.: Wallingford, CT, 2004.
- (13) Thomas, J. A.; Young, J. W.; Fleisher, A. J.; Alvarez-Valtierra, L.; Pratt, D. W. *J. Phys. Chem. Lett.* **2010**, *1*, 2017.
- (14) Rode, M. F.; Sobolewski, A. L. *Chem. Phys.* **2008**, *347*, 413.
- (15) Marks, D.; Zhang, H.; Borowicz, P.; Waluk, J.; Glasbeek, M. *J. Phys. Chem. A* **2000**, *104*, 7167.
- (16) Kina, D.; Nakayama, A.; Noro, T.; Taketsugu, T.; Gordon, M. S. *J. Phys. Chem. A* **2008**, *112*, 9675.
- (17) Young, J. W.; Pratt, D. W. *J. Chem. Phys.* **2011**, in press.
- (18) Brand, Chr.; Kuepper, J.; Pratt, D. W.; Meerts, W. L.; Kruegler, D.; Tatchen, J.; Schmitt, M. *Phys. Chem. Chem. Phys.* **2010**, *12*, 4968 and the following paper.
- (19) See, for example, Sytnik, A.; Gormin, D.; Kasha, M. *Proc. Natl. Acad. Sci. U.S.A.* **1994**, *91*, 11968.
- (20) Young, J. W.; Fleisher, A. J.; Pratt, D. W. *J. Chem. Phys.* **2011**, *134*, 084310.